

SENSITIVITY ANALYSIS OF PREDICTED CONVECTIVE HEAT TRANSFER AT INTERNAL BUILDING SURFACES TO DIFFUSER MODELLING IN CFD

Kim Goethals¹ and Arnold Janssens¹
¹Ghent University, Ghent, Belgium

ABSTRACT

As a cost-effective alternative to experiments, computational fluid dynamics (CFD) can provide new insight in airflow patterns and the related convective heat transfer (CHT). However, together with the governing equations, the description of the boundary conditions determines for a greater part the reliability and the accuracy of CFD simulations. In this study the sensitivity of the predicted CHT to diffuser modelling is studied. Numerical simulations of a modified version of test case E.2 of the IEA Annex 20-project are performed. The results show a strong influence of the applied diffuser model on the predicted CHT.

INTRODUCTION

To predict the building performance in detail, one could consider to solve the conservation equations for the temperature and velocity fields. However, high computational costs and the necessity of considerable empiricism limit the use of computational fluid dynamics (CFD) in building design, in favour of multi-zone energy simulation (ES). Yet, a key parameter of building performance analysis using ES is the prediction of interior convective heat transfer (CHT): the choice of the CHT algorithm is of the same importance as the choice of the design parameters, such as internal heat gains or sun blind control (Goethals and Janssens, 2008). Clearly, more accurate approaches for the range of flow regimes experienced within buildings are required in ES. Moreover, CHT modelling should adapt to changes in the flow by selecting an appropriate CHT algorithm.

As a cost-effective alternative to experiments, CFD can provide new insight in indoor airflow patterns and the related CHT. However, experience indicates the limitations of the currently available CFD results. Together with the governing equations, the description of the boundary conditions determines for the greater part the reliability and the accuracy of CFD simulations, as identified in the IEA Annex 20-project (Lemaire, 1993). Moreover, it is not easy to handle all the boundary conditions with a high level of accuracy. Especially the air supply opening may cause problems. Because of the large scale-difference between the diffuser and the room, it is necessary to

make an approximation and simplification of the supply geometry, admitting the use of a coarser mesh. The different solutions which can be applied to model a diffuser, can be divided into two groups. In the first approach, the initial jet momentum of the diffuser is imposed directly at the supply opening. This group includes the simplified geometrical model (SGM) and the momentum model (MM). On the other hand, the box model (BM) and the prescribed velocity model (PVM) are part of the momentum modelling in front of the air supply diffuser plane.

Numerical simulations of a modified version of test case E.2 of the IEA Annex 20-project are performed using CFD. To evaluate the sensitivity of the predicted CHT to diffuser modelling, the above-mentioned models are applied to simulate the complex HESCO-type nozzle diffuser.

EXPERIMENT SETUP

The test room of the IEA Annex 20-project has internal dimensions of 4.2m x 3.6m x 2.5m – as shown in Figure 1. In the front wall a HESCO nozzle diffuser is mounted 0.20m below the ceiling, symmetrically placed between the side walls. It consists of 84 round nozzles that are arranged in four identical rows in an area of 0.71m x 0.17m. The flow direction of each nozzle is adjusted with an angle 40° upwards. The ventilation rate of the room is 3 air changes per hour (ach) while the supply air temperature is 15°C. On the same wall an outlet – 0.30m wide and 0.20m high – is located 1.7m above the floor. Contrary to the original setup, the window on the opposite wall is omitted to reduce the complexity. In this case all surroundings are kept at 21°C.

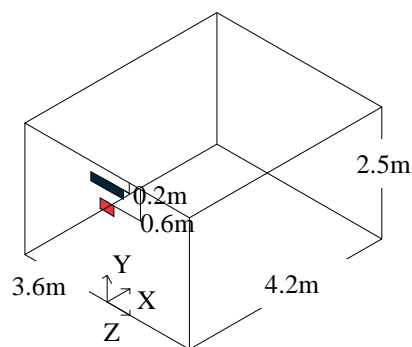


Figure 1 Configuration of the test room

SIMULATION APPROACH

Grid

Since most experimental cases used to determine the CHT correlations are three-dimensional, the simulations are also conducted for a three-dimensional model. However, the number of grid cells, read into the commercial solver Fluent 6.2 (Fluent, 2005), is limited by using a symmetric condition for the transversal section. The shown flow asymmetry (Fossdal, 1990, Luo et al., 2004) is of little account, because an inter-model comparison of the diffuser models will be performed.

Obviously, the results depend crucially on the grid. Therefore, the grid has to be designed in such a manner that it does not introduce errors that are too large. Firstly, this means that the grid quality should be high: the use of hexahedral cells – known to introduce smaller truncation errors and display better convergence than tetrahedral (Hirsch et al., 2002) – and limited stretching/compression in regions of high gradients. In addition, the resolution should be fine enough to capture the important phenomena like shear layers and vortices. The necessary resolution has to be analyzed using a systematic grid convergence study. To estimate the discretization error and uncertainty, generalized Richardson extrapolation should be tried, as it is the most general error estimation approach. Numerical errors due to computer programming, round-off or incomplete iterative convergence are assumed to have been reduced to a negligible amount. The principle and the limitations of Richardson extrapolation as applicable to CFD codes using time-averaged flow equations are extensively described in, amongst others, Roache (1998), Stern et al. (2001) and Franke et al. (2007).

For Richardson extrapolation, solutions f_i on at least three systematically refined/coarsened grids are necessary, using a refinement ratio r , giving a triplet. In this case $i=1$ denotes the fine, $i=2$ the medium and $i=3$ the coarse grid. Firstly, monotonic convergence is considered necessary. From the ratio of the solution changes R (1), three behaviours can be discerned – as shown in (2):

$$R = \frac{(f_2 - f_1)}{(f_3 - f_2)} \quad (1)$$

$$\begin{aligned} 0 < R < 1 & \quad : \text{monotonic convergence} \\ R < 0 & \quad : \text{oscillatory convergence} \\ |R| > 1 & \quad : \text{divergence} \end{aligned} \quad (2)$$

For divergence, errors and uncertainties cannot be estimated. In case of oscillatory behaviour, only the uncertainties of the errors can be estimated, not the signs and magnitudes. To compute an uncertainty band, upper and lower bounds of solution oscillation have to be derived on more than three grids. A second condition for the applicability of Richardson

extrapolation is that the solutions on the three meshes are in the asymptotic range, which is examined as follows. Assuming monotonic convergence, the observed order of accuracy is calculated (3):

$$p = \frac{\ln[(f_3 - f_2)/(f_2 - f_1)]}{\ln(r)} \quad (3)$$

Using the estimate of the exact solution (4), based on the two finest grids, relation (5) has to be valid for the solutions to be in the asymptotic range.

$$f_{ex} = f_1 + \frac{(f_1 - f_2)}{r^p - 1} \quad (4)$$

$$f_1 - f_{ex} = \frac{f_2 - f_{ex}}{r^p} = \frac{f_3 - f_{ex}}{r^{2p}} \quad (5)$$

The most common approach with Richardson extrapolation in grid convergence studies is to calculate the relative error $|E_i|$. This is generally done for the solution on the fine grid – as shown in (6).

$$|E_1| = \frac{1}{r^p - 1} \left| \frac{f_2 - f_1}{f_1} \right| \quad (6)$$

The magnitude of the relative error defines an error band around the solution on the grid, i.e. $f_1(1 \pm |E_1|)$. This definition, however, provides only 50% confidence (Roy, 2005). Therefore, the relative error is in general multiplied by a safety factor. The choice of the appropriate safety factor is a matter of ongoing discussion (e.g. Stern et al., 2001, Roache, 2002). In this study, the safety factor as described by Roache (1998) is used, i.e. 1.25, since the error band is calculated only when the solutions, obtained on three meshes, are in the asymptotic range.

Only the SGM is used to find the proper grid resolution, which is assumed to be applicable for the other diffuser models. The flow field is computed on three grids which are systematically coarsened twice, resulting in three triplets. In accordance with the different proposed minimum values of the refinement ratio (Roache, 1998; Stern et al., 2001; Ferziger and Peric, 2002), a constant non-integer value of 1.5 is chosen, since halving the grid may put the solution out of the asymptotic range. As Richardson extrapolation can be applied to local flow variables as well as to derived integral quantities, the velocity magnitude v_j and the temperature T_j at two locations $j - a(1,4,2,0)$ and $b(3,2,0)$ – and the CHT coefficient (CHTC) at the ceiling are investigated. To derive the CHTC, a reference temperature has to be defined – consistent with the definition of CHT (7):

$$q = CHTC(T_s - T_{ref}) \quad (7)$$

The choice of the reference temperature depends on the ventilation regime: the supply, the local or the room air temperature. As suggested by Novoselac

(2005), the local air temperature is used which comprises the mass-averaged temperature of the parallel layer of 0.1m thickness, 0.1m away from the surface. In line with the ratio of the solution changes, Richardson extrapolation can be applied only for T_a and CHTC using the finest grid triplet – as shown in Table 1. As for the remaining variables, oscillatory or divergent behaviour is observed.

Table 1
Ratio of solution changes R (-)

TRIPLET	v_A	T_A	v_B	T_B	CHTC
144x81x63	-0.6	-0.6	-0.6	-0.9	-0.8
162x99x72	2.8	-11.1	38.0	-20.1	3.2
171x99x72	-0.7	0.01	-0.2	-0.04	0.1

Since the CHTC is the primary object of investigation, the finest grid of the third triplet is considered appropriate, taking a relative error of 2% into account.

Turbulence modelling

Almost all room airflows are turbulent, which has a big influence on the fluid motion. However, resolving the time-dependent Navier-Stokes equations for high Reynolds-number turbulent flows in complex geometries all the way down to the smallest scales is unlikely to be practical for some time to come. Currently, the use of turbulence models for mean flow is appraised. Unfortunately, no single turbulence model is universally accepted as being superior for all classes of problems. For the prediction of two-dimensional ventilation flows, Chen (1995) compared the performance of five k- ϵ turbulence models in predicting natural convection, forced convection and mixed convection in rooms, as well as impinging jet flow. Among them, the ReNormalization Group (RNG) k- ϵ model gives the best overall results. In accordance with this finding, Buchanan (1997) and Loomans (1998) adopted the RNG k- ϵ turbulence model for their three-dimensional indoor airflow studies: a good correlation of the predictions with experimental data was found. Also Gan (1998) recommended the use of this model to predict buoyancy-induced airflows in rooms. Moreover, for a similar – however isothermal – experimental setup as the one under consideration, Luo and Roux (2004) found that the RNG k- ϵ model yields a good prediction for the wall jet flow issued from the HESCO nozzle diffuser. The study showed also that the model is very robust and the calculation converges smoothly. As pointed out earlier by Chen (1996), no significant better results were obtained using the computational more demanding Reynolds Stress Model.

The RNG method shows the best overall performance of the k- ϵ models, because it provides a low-Reynolds number interpolation formula for the turbulent viscosity, which is valid for low- to high-

Reynolds number flows. Effective use of this feature, however, depends on an appropriate treatment of the near-wall treatment. While the k- ϵ model is only valid for fully turbulent flows, there are two ways to make the k- ϵ model suitable for wall-bounded flows: with wall functions or with low-Reynolds models, also known as enhanced wall treatment. The wall functions intend to reproduce the derived logarithmic velocity profile of typical forced convection boundary layer flows and are therefore not applicable for natural and mixed convection flows. In the low-Reynolds approach the k- ϵ equations are modified in order to make them valid throughout the full range of the flow region and the near-wall region is resolved all the way down to the wall. As concluded by Awbi (1998), the enhanced wall treatment – as applied in this study – gives better agreement with the experimentally derived CHTC.

Boundary conditions: surface boundary

Alongside the governing equations, the boundary conditions determine to a large extent the reliability and the accuracy of CFD predictions – as mentioned above. When CFD is used only for indoor airflow prediction, the user needs to define the following boundary conditions: convective heat flux or surface temperature at enclosure surfaces and the flow entering or leaving the room at wall openings.

The wall boundary conditions are used to bound fluid and solid regions. In viscous flows, the no-slip boundary condition, i.e. zero velocities, is specified at walls by default in Fluent. Meanwhile, a temperature of 21°C is imposed.

Boundary conditions: air supply diffuser

In the IEA Annex 20-project, Heikkinen (1991) originally represented the HESCO nozzle diffuser as a single rectangular opening with the same effective flow area and aspect ratio as the real diffuser which is located in the centre of the diffuser, known as the SGM. The effective area is the net area of a diffuser utilized by the air stream. As observed by Skovgaard and Nielsen (1991), the effective inlet area is a function of the air change rate. For a ventilation rate of 3ach, the effective flow area of the nozzle diffuser is 0.00855m². However, Heikkinen proposed greater dimensions of 180mm width and 62mm height to get approximately the same maximum velocity at the opening as in the nozzles – as applied in this study. The inlet opening is described by an ‘inlet velocity boundary condition’. The supply velocity is 3.68m/s and the flow is directed upwards at an angle of 40°. Corresponding with a turbulence intensity of 10%, the turbulence kinetic energy k is 0.204m²/s² and its dissipation rate ϵ 6.65m²/s³. Further tests with higher turbulence intensities of 15% and 20% were carried out for the isothermal setup by Luo and Roux (2004). However, no significant influence was found for the predicted results, which corresponds with the results reported by Awbi (1989).

Through the same international effort, IEA Annex 20, Chen and Moser (1991) developed the MM. In this case, the diffuser is simulated as an opening with the same gross area, mass inflow and momentum flux as the real diffuser. The air supply velocity for the momentum source term is calculated by using the effective area. To ensure the correct mass and momentum flows, the mass and momentum boundary conditions for the diffuser were originally separately described. However, most commercial CFD packages, such as Fluent, do not support the separate description of boundary conditions for continuity and momentum equations. Therefore, a momentum source is added to a volume adjacent to the diffuser while the total mass flow rate and the flow direction are specified at the supply opening – as shown in Figure 2. As proposed by Chen and Moser (1991), the opening has a dimension of 0.355m width – since only half of the room is modelled – and 0.135m height and is located 2.13m above the floor.

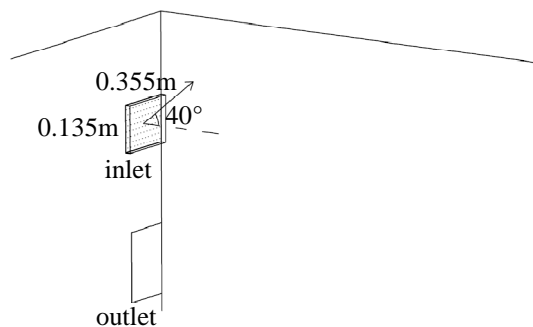


Figure 2 Momentum model

The momentum force of the added source is determined by the difference between the effective momentum and the momentum originating from the simplified opening. The momentum force F is described by (9). In this equation v represents the velocity magnitude at the exit of the nozzle opening in case of the effective momentum, respectively the simplified gross outflow surface. In the former case, A corresponds with the effective area, while in the latter, A stands for the gross area.

$$F = \int \rho v^2 dA \quad (9)$$

To define a source of momentum in Fluent, the momentum force is set for a given volume in the momentum conservation equation (Fluent 2005). Obviously, the volume of the momentum source cell is an important parameter for the correct prediction of the wall jet flow issued from the nozzle diffuser. To determine the optimum dimension Luo and Roux (2004) compared the predicted velocity profiles with different momentum source cell sizes. They recommend that for a ventilation rate of 3ach, the dimension of the momentum source cell in the stream wise direction should be in the range of 0.014-0.018m. In this study, a value of 0.015m is used.

In the BM, developed by Nielsen (1973), the diffuser boundary condition is specified on an imaginary box surface around the diffuser while the flow field inside the box is ignored – as shown in Figure 3.

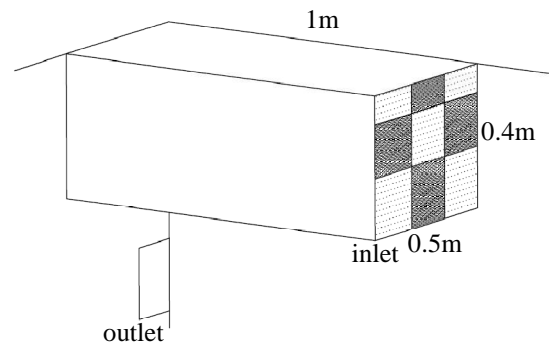


Figure 3 Box model

Originally, the BM uses distributions of air velocity, air temperature and contaminant concentrations at the surface in front of the diffuser. On the other surfaces a free boundary with zero gradients in the normal direction of the surfaces for flow parameters (velocity, temperature concentration, etc.) is specified. However, Srebric (2000) and Srebric and Chen (2001) found that the resulting distributions of air temperature and tracer-gas concentration in a room are insensitive to the profiles of the temperature and contaminant concentration distributions at the box surface. Therefore, only the velocity profile – possibly obtained under isothermal conditions – needs to be specified while the other parameters can be set as uniform. In addition to the velocity distribution, the box size is another important parameter. If the diffuser discharges multiple jets, such as the nozzle diffuser, the front surface of the box should be in the region where the diffuser jets have merged. At the same time, the box has to be sufficiently small to avoid the impact of room air circulation and thermal plumes on the jet (Srebric and Chen, 2000). The minimal box size can be roughly estimated from smoke visualization. A practical way, however, is to define the box surface at a location where the buoyancy force is negligible compared to the momentum force, defined by the local Archimedes number (Grimtlyn and Pozin 1993). In this study, the box size, also used by Heikkinen (1991), Ewert et al. (1991) and Srebric (2000), is 1.0m x 0.5m x 0.4m. The velocity profiles measured by Heikkinen (1991) – displayed in Figure 4 – are used to set the boundary conditions for the front box surface. The data shows that the jet has a very strong three-dimensional feature. Analogous to Srebric and Chen (2001), the front surface is divided in 3x3 patches, each using a normal velocity averaged from the measured data for the represented area. In the mean time, the patches are defined by the same turbulence quantities and temperature as in the previous two models. The other surfaces of the box are defined as a ‘symmetry’ plane.

Table 2
Material properties for air at 20°C

PROPERTY	VALUE
ρ [kg/m ³]	1.205
C_p [J/kgK]	1006.094
λ [W/mK]	0.02570262
ν [kg/ms]	$1.81349 \cdot 10^{-5}$
β [1/K]	0.00343

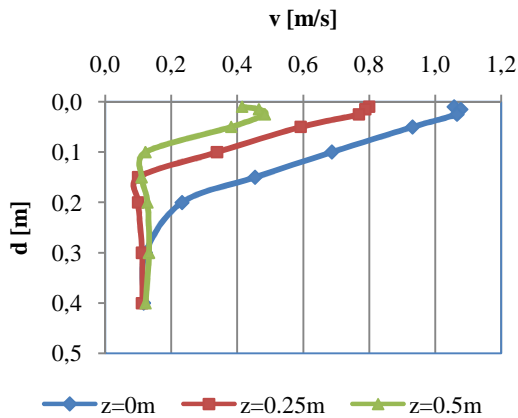


Figure 4 Measured velocity profiles

The PVM was developed by Gosman et al. (1980) to reduce the number of measurements needed for the BM. In this model the boundary conditions are given at a simple opening analogous to the SGM. In addition, data is also defined at some critical locations around the diffuser. These values are used to correct the predicted values around the diffuser. In this study only the x-direction velocity was specified in a plane similar to the front surface of the BM above. The present version of the method means a simplification of the method described in Nielsen (1989).

Boundary conditions: air exit opening

The exhaust opening is represented by a 'pressure outlet boundary condition'. At the opening the gauge pressure is set as zero using the Dirichlet condition. This type of boundary condition specifies the values a solution needs to take on the boundary of the domain. Luo and Roux (2004) also tested the Neumann condition, which specifies the values that the derivative of a solution is to take on the boundary. They found no difference between the predicted results in these two methods. Fluent (2005) recommends the Dirichlet condition as it offers better stability and convergence. The inlet turbulence intensity is assumed to be 10% as recommended by, amongst others, Ewert et al. (1991) and Skovgaard and Nielsen (1991).

Material properties

Table 2 shows the used material properties of the indoor air at an estimated temperature of 20°C. For modelling buoyancy, Fluent (2005) proposes two ways: transient calculation or steady-state calculations using the Boussinesq model. Since the temperature difference in the experimental setup is not too large, the last approach, which reaches faster convergence, is recommended by Fluent (2005). This method treats density as a constant value in all solved equations, except for the buoyancy term in the momentum equation.

Numerical procedure

In the finite volume method, the approach used to linearize and solve the discretized equations should be determined. Because of limited computational power, the segregated solver is used in this study: the equations are solved sequentially.

Besides, it is necessary to replace the values at the cell surfaces with values at the grid points and to obtain a final version of the discretization equation. This requires an interpolation from the variable value at the cell centre to the cell faces. Different interpolation schemes are made over the years. For all the convection terms the second-order upwind scheme is used. Luo and Roux (2004) also tested the QUICK scheme – a higher-order differencing scheme – and found a great degradation of the predicted results. Moreover, the QUICK scheme is more difficult to converge, which was also observed by Srebric and Chen (2000). The pressure-velocity coupling is made by the SIMPLE algorithm and for the discretization of pressure the PRESTO scheme is applied.

Because of the non-linearity of the problem the segregated solver uses under-relaxation to control the update of computed variables at each iteration. In Fluent, the default under-relaxation parameters for all variables are set to values that are near optimal for the largest possible number of cases. However, for the case at hand, mixed convection, they are not suitable. Therefore, the under-relaxation factors are modified consistent with Fluent recommendations (Fluent 2005) – as shown in table 3.

Table 3
Used under-relaxation factors

PROPERTY	VALUE
Pressure	0.2
Density	0.8
Body forces	1
Momentum	0.5
k	0.5
ϵ	0.5
Turbulent viscosity	1
Energy	0.8

RESULTS AND DISCUSSION

Influence of diffuser model on the predicted CHT

Figure 4 compares the simulated CHTC at three enclosure walls for the different diffuser models. In addition to the absolute values, the CHTC is expressed relative to the solutions obtained with the BM. Consistent with Srebric and Chen (2000), the BM is considered the most appropriate simplification of the nozzle diffuser, in spite of an over prediction of the maximum jet velocity by 25%. The predicted CHTC deviates up to 64% from the results obtained with the BM. Overall, the SGM produces the highest CHTC, supposedly because this method simulates a diffuser with a very small jet area, which limits the decay. Different from Srebric and Chen (2000), the MM and the BM give very different CHTC values. When comparing the calculated and measured velocities the last-mentioned authors found a good agreement. However, in this study, the MM is defined by a source cell instead of by a separate description of mass and momentum equations. Moreover, no local grid refinement is used – as recommended by Luo and Roux (2004). As for the PVM, the results are not very different from those of the BM. This probably originates from the similar definition of the velocity magnitude.

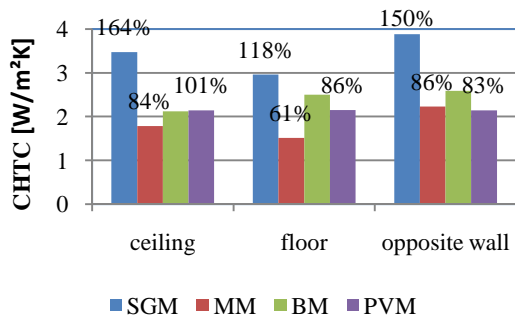


Figure 4 CHTC at three enclosure walls for different diffuser models

Comparison of simulated heat fluxes with those of CHTC correlations

In addition to the inter-model analysis of the CHTC prediction, the calculated results are compared with empirical correlations. As found in literature, different authors have developed correlations for various flow regimes. In case of natural convection, the CHTC is a function of the temperature difference between the concerned surface and the air – as shown in equation (10). For horizontal surfaces, the CHTC also depends on the flow direction.

$$CHTC_{natural} = C(\Delta\theta)^n \quad (10)$$

In equation (10), C and n are semi-empirical coefficients, which were determined by, amongst others, Alamdari and Hammond (1983), and Awbi and Hatton (1999). Furthermore, authors like Fisher

(1995) and Pederson (1997) have derived correlations for forced convection as a function of the airflow rate. Finally, to characterize mixed convection – representative for the case at hand – above-mentioned CHTCs can be combined using the asymptotic approach of Churchill and Usagi (1972), as described by Beausoleil-Morrison (2000):

$$CHTC_{mixed} = \left(CHTC_{natural}^n + CHTC_{forced}^n \right)^{1/n} \quad (11)$$

Furthermore, also Awbi and Hatton (2000) and Novoselac (2005) have tested configurations where both mechanical and buoyant forces are important.

In this study the simulated results are compared with the above-mentioned correlations applicable for natural convection – Alamdari and Hammond (1983) and Awbi and Hatton (1999) represented by A&H(1983), respectively A&H (1999) – and the mixed convection CHTCs derived by Awbi and Hatton (2000) and Beausoleil-Morrison (2000) – identified by A&H (2000) and B (2000). The comparison is straightforward because of the use of the same reference temperature, i.e. the local air temperature. In Figure 5 and 6, the convective heat flux is plotted as a function of the temperature difference between the concerned surface and the local air. As observed above, the SGM over predicts the CHT. The predicted results of the MM yield closer to the correlations. However, both the temperature difference and the convective heat flux are considerably smaller than the values obtained with the other models. Meanwhile, the heat flux of the BM and PVM lie closest to the values obtained with Beausoleil-Morrison. This algorithm can be regarded as the most appropriate because it takes the interaction, i.e. assisting or opposing, of natural and forced convection into account. The prediction of a high CHT at low temperature differences is due to the scaling of the forced convection algorithm which originally uses the diffuser temperature as reference, instead of the local air temperature.

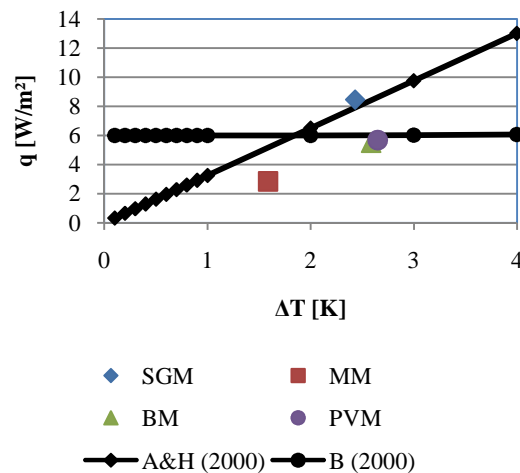


Figure 5 Convective heat flux at the ceiling: empirical correlations and simulated values

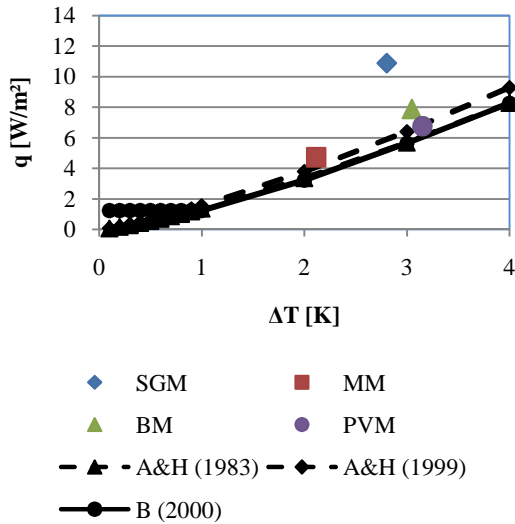


Figure 6 Convective heat flux at the opposite wall: empirical correlations and simulated values

CONCLUSION

This study has shown that grid independence is difficultly obtained, considering the current computational limits. Only a derived integral quantity, like e.g. the averaged CHTC at a surface, can be estimated using generalized Richardson extrapolation. Meanwhile, the prediction of the convective heat flux depends strongly on the diffuser modelling method. The CHT predicted by the BM corresponds reasonably well with the result obtained with the convection algorithm of Beausoleil-Morrison (2000), which is regarded the most appropriate for the case at hand. As for the other diffuser modelling methods, the predicted CHTC deviates up to more than 50%. Bearing the sensitivity of thermal predictions to internal CHT – discussed in Goethals and Janssens (2008) – in mind, this deviation is unacceptable. Therefore, a correct modelling of the used diffuser is primary in deriving the CHTC.

ACKNOWLEDGEMENT

This work was funded by the Institute for the Promotion of Innovations through Science and Technology in Flanders (project IWT-050154).

NOMENCLATURE

$ E_i $	relative error on grid i	
A	area	[m ²]
C	semi-empirical coefficient	
F	momentum force	[N]
f_{ex}	exact numerical solution	
f_i	solution on grid i	
k	turbulence kinetic energy	[m ² /s ²]
n	semi-empirical coefficient	
p	observed order of accuracy	[-]
q	convective heat flux	[W/m ²]
R	ratio of solution changes	[-]

r	refinement ratio	[-]
T_j	temperature at point j	[K]
v_j	velocity magnitude at point j	[m/s]
ϵ	turbulence dissipation rate	[m ² /s ³]
ρ	air density	[kg/m ³]

REFERENCES

- Alamdari, F. and Hammond, G.P. 1983. Improved data correlations for buoyancy-driven convection in rooms, *Building Services Engineering Research and Technology*, 4(3), pp.106-112.
- Awbi, H.B. 1989. Application of computational fluid dynamics in room ventilation, *Building and environment*, 24(1), pp.73-84.
- Awbi, H.B. 1998. Calculation of convective heat transfer coefficients of room surfaces for natural convection, *Energy and Buildings*, 28(2), pp.219-227.
- Awbi, H.B. and Hatton, A. 1999. Natural convection from heated room surfaces, *Energy and Buildings*, 30(3), pp.233-244.
- Awbi, H.B. and Hatton, A. 2000. Mixed convection from heated room surfaces, *Energy and Buildings*, 32(2), pp.153-166.
- Beausoleil-Morrison, I. 2000. The adaptive coupling of heat and airflow modelling within dynamic whole-building simulation, University of Strathclyde, Glasgow, United Kingdom, Ph D.
- Buchanan, C.R. 1997. CFD characterization of a mechanically ventilated office room: the effects of room design on ventilation performance, University of California, California, USA, Ph D.
- Chen, Q. 1995. Comparison of different k-e models for indoor airflow computations, *Numerical Heat Transfer Part B*, 28, pp.353-369.
- Chen, Q. and Moser, A. 1991. Simulation of a multiple nozzle diffuser, Ottawa, Canada, Proceedings of 12th AIVC conference, pp.1-14.
- Chen, Q. et al. 1996. Simulation of a complex air diffuser with CFD technique, Fifth international conference on air distribution in rooms, Roomvent '96, 1, pp.227-234.
- Ewert, M., Renz, U., Vogl, N. and Zeller, M. 1991. Definition of the flow parameters at the room inlet devices – measurements and calculations, Proceedings of 12th AIVC conference, Ottawa, Canada, pp.231-237.
- Ferziger, J.H. and Peric, M. 2002. Computational methods for fluid dynamics, Springer Verlag, Berlin Heidelberg, New York, 3rd edition.
- Fisher D.E.. 1995. An experimental investigation of mixed convection heat transfer in a rectangular enclosure. University of Illinois, USA, PhD.

- Fisher D.E. and Pederson C.O. 1997. Convective heat transfer in building energy and thermal load calculations. *ASHRAE Transactions*, 103(2), pp.137-148.
- Fluent. 2005. *Fluent's user guide – Version 6.1*, Fluent Inc., Lebanon, USA.
- Fossdal, S. 1990. Measurement of test case E – mixed convection, summer cooling, Preliminary report of International Energy Agency Annex 20.
- Franke, J., Hellsten, A., Schlünzen, H. and Carissimo, B. 2007. *COST – Best practice guideline for the CFD simulation of flows in the urban environment*, University of Hamburg, Hamburg, Germany.
- Gan, G. 1998. Prediction of turbulent buoyant flow using an RNG k- ϵ model, *Numerical Heat Transfer Part A*, 33, pp.169-189.
- Goethals, K. and Janssens, A. 2008. Sensitivity analysis of thermal prediction to convective heat transfer at internal surfaces, Leuven, Belgium, *Proceedings of the Building Physics Symposium 2008*, pp. 147-150.
- Gosman, A.D, Nielsen, P.V., Restivo, A. and Whitelaw, J.H. 1980. The flow properties of rooms with small ventilation openings, *Transactions of the ASME*, 102, pp.316-323.
- Grimitlyn, M.I. and Pozin, G.M. 1993. Fundamentals of optimizing air distribution in ventilated spaces, *ASHRAE Transactions*, 99(1), pp.1128-1138.
- Heikkinen, J. 1991. Modelling of supply air terminal for room airflow simulation, *Proceedings of 12th AIVC conference*, Ottawa, Canada, pp.24-27.
- Hirsch, C., Bouffieux V. and Wilquem, F. 2002. CFD simulation of the impact of new buildings on wind comfort in an urban area, in Augusti, G., Borri, C. and Sacré, C., editors, *Impact of wind and storm on city life and built environment*, *Proceedings of the workshop*, CSTB, Nantes, France, pp.164-171.
- Lemaire, A.D. 1993. Annex 20 – Airflow patterns within building. Room air and contaminant flow – Evaluation of computational methods, TNO Building and Construction Research, Delft, the Netherlands.
- Loomans, M.G.L.C. 1998. The measurement and simulation of indoor airflow, Eindhoven University of technology, Eindhoven, the Netherlands, Ph D.
- Luo, S. and Roux, B. 2004. Modeling of the HESCO nozzle diffuser used in IEA Annex 20 experiment test room, *Building and Environment*, 39, pp.367-384.
- Luo, S., Heikkinen, J. and Roux, B. 2004. Simulation of airflow in the IEA Annex 20 test room – validation of a simplified model for the nozzle diffuser in isothermal test cases. *Building and Environment*, 39, pp.1403-1415.
- Nielsen, P.V. 1973. Berechnung der Luftbewegung in einem zwangsbelüfteten Raum, *Gesundheits-Ingenieur*, 94, pp.299-302.
- Nielsen, P.V. 1989. Representation of boundary conditions at supply openings, IEA Annex 20, Internal report, University of Aalborg, Aalborg, Denmark.
- Novoselac, A. 2005. Combined airflow and energy simulation program for building mechanical system design. Pennsylvania State University, USA, Ph D.
- Roache, P.J. 1998. *Verification and validation in computational science and engineering*, Hermosa Publishers, New Mexico, Mexico.
- Roache, P.J. 2002. Recent contributions to verification and validation methodology. *Proceedings of the fifth world congress on computational mechanics*, Vienna University of Technology, Austria.
- Roy, C.J. 2005. Review of code and solution verification procedures for computational simulation, *Journal of Computational Physics*, 205, pp.131-156.
- Skovgaard, M. and Nielsen, P.V. 1991. Modelling complex geometries in CFD – applied to air ventilated rooms, *Proceedings of 12th AIVC conference*, Ottawa, Canada, pp.183-200.
- Srebric, J. 2000. Simplified methodology for indoor environment design, Massachusetts institute of technology, Cambridge, USA, PhD.
- Srebric, J. and Chen, Q. 2000. Simplified diffuser boundary conditions for numerical room airflow models, Final report for ASHRAE RP-1009, Massachusetts Institute of Technology, Cambridge, USA.
- Srebric, J. and Chen, Q. 2001. A method of test to obtain diffuser data for CFD modelling of room airflow, *ASHRAE Transactions*, 107(2), pp.108-116.
- Stern, F., Wilson, R.V., Coleman, H.W. and Paterson, E.G. 2001. Comprehensive approach to verification and validation of CFD simulation – Part 1: Methodology and Procedures, *ASME Journal of Fluids Engineering*, 123, pp.793-802.